Published in "Dalton Transactions 41: 5570-5576, 2008"
which should be cited to refer to this work.

Probing the potential of *N*-heterocyclic carbenes in molecular electronics: redox-active metal centers interlinked by a rigid ditopic carbene ligand

Laszlo Mercs,[a] Antonia Neels[b] and Martin Albrecht*[a]

Bimetallic homonuclear iron(II) and ruthenium(II) *N*-heterocyclic carbene complexes have been synthesized and crystallographically analyzed. As a spacer ligand for interconnecting the two redox-active metal centers, a ditopic carbene ligand has been used that comprises two carbene sites annelated to benzene. Detailed electrochemical and spectroelectrochemical analyses of the bimetallic systems revealed that despite the potentially π-delocalized nature of the ditopic ligand, the iron centers are only moderately coupled. In the ruthenium complexes, the intermetallic interactions are very weak and the centers are electrochemically nearly independent. A model is proposed for rationalizing these observations which is based on (i) relatively weak charge delocalization in the spacer ligand and (ii) on electrostatic factors governing the metal–carbene bond.

http://doc.rero.ch

Introduction

The development of *N*-heterocyclic carbenes (NHCs) as ligands for transition metal chemistry has had a major impact on catalysis.[1] The application of these ligands in other areas of materials science has, however, been much less developed.[2] This is remarkable, in particular given the unique bonding properties of NHCs that invoke unprecedented activities of the coordinated metal center. Extensive theoretical and experimental analyses of the NHC bonding to transition metals has revealed intriguing features: While the strong σ donor properties of NHC ligands have been undisputed,[3] recent results have also shown that metal-to-carbene π backbonding is significant, especially[4] when the NHC ligand is coordinated to d^6 or d^8 metal centers.[5,6] A recent experimental study demonstrates that π-active substituents attached to the remote C(4) carbon of 2-imidazolylidenes can be used for tuning the electronics of the metal center, possibly *via* long-range mesomeric interactions between the metal center and the substituent.[7]

This apparently favorable orbital organisation within the NHC ligand and the partial π character of the metal–ligand bond presets NHCs as potential linkers between electronically active sites.[8] Efficient through-bond electronic coupling of the redox-partners allows mixed-valent states to be accessible in addition to the fully oxidized and reduced states (superexchange model).[9] A high degree of intermetallic coupling is pivotal for addressing the different states and is typically achieved by rigid, π-conjugated spacer ligands. The dicarbene **A**, derived from the corresponding diimidazolium salt (Scheme 1) as pioneered by Bielawski and coworkers,[10] should fulfill these requirements for a spacer.

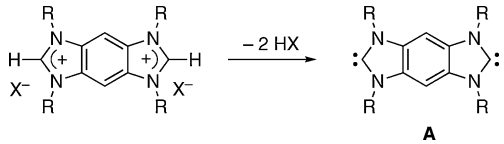

Scheme 1 Synthesis of the ditopic free carbene spacer ligand **A**.

Specifically, dicarbenes such as **A** comprise (i) two bonding sites for metal coordination, (ii) a π-conjugated linker between the two carbene bonding sites, and (iii) considerable metal–carbon π interactions when bound to redox active iron(II) centers.[5] In addition, the M–C bond is robust and tolerates air and moisture in most cases, which is beneficial for the application of such complexes in functional materials.

Here we report on the potential of this type of ditopic ligand in coupling two redox active iron and ruthenium centers. Contrary to our expectations, electrochemical analyses and comparative studies using analogous monometallic carbene complexes indicate that intermetallic coupling is only weak, in particular in the diruthenium complexes.

Experimental

General

All reactions have been performed using standard Schlenk techniques under an argon atmosphere unless stated otherwise. Toluene, THF and CH_2Cl_2 were dried by passage through solvent purification columns, all other reagents were used without further purification. The benzdiimidazolium salt **1** was prepared according to published methods[2a] and subjected to ion exchange using Dowex 1×2–200 chloride exchange resin in MeOH.[11] The synthesis of dibutylimidazolium bromide **4** has been described elsewhere.[12] All ^1H and $^{13}C\{^1H\}$ NMR spectra were recorded on Bruker Avance spectrometers operating at 400 or 500 MHz (^1H NMR) and 100 or 125 MHz (^{13}C NMR), respectively. Chemical

[a]*Department of Chemistry, University of Fribourg, Chemin du Musee 9, CH-1700, Fribourg, Switzerland. E-mail: martin.albrecht@unifr. ch; Fax: +41 263009738; Tel: +41 263008786*
[b]*Institute of Microtechology, University of Neuchâtel, Rue Jaquet Droz 1, CH-2002, Neuchâtel, Switzerland*

shifts (δ) are given in ppm and were referenced to residual solvent ^{1}H or ^{13}C resonances (coupling constants J in Hz). Assignments are based either on distortionless enhancement of polarization transfer (DEPT) experiments or on homo- and heteronuclear shift correlation spectroscopy. IR spectra were recorded on a Mattson 5000 FTIR instrument in CH_2Cl_2 solution. Elemental analyses were performed by the Microanalytical Laboratory of Ilse Beetz (Kronach, Germany) and by the Microanalytical Laboratory of the ETH Zürich (Switzerland). A commercially available Hg lamp was used for irradiation.

Synthesis

Complex 2. To a suspension of the benzdiimidazolium salt **1** (114 mg, 0.25 mmol) in dry THF (5 mL) was added $LiN(SiMe_3)_2$ (1 M in THF, 0.5 mL, 0.5 mmol) at room temperature. After stirring for 1 h, this solution was added to a solution of $[FeI(cp)(CO)_2]$ (144 mg, 0.48 mmol) in dry toluene (5 mL) and stirring was continued for 16 h. The formed precipitate was separated by centrifugation, washed once with dry toluene (10 mL) and then extracted with dry CH_2Cl_2 (3 × 20 mL). The combined CH_2Cl_2 fractions were reduced to *ca.* 20 mL and subsequently irradiated for 16 h. All volatiles were removed *in vacuo*, and the residue was purified by column chromatography (SiO_2, CH_2Cl_2). The product was obtained as a green powder (62 mg, 28%). X-Ray quality crystals were grown by slow diffusion of pentane into a CH_2Cl_2 solution of **2** at –20 °C. ^{1}H NMR (C_6D_6, 400 MHz, 283 K): δ 7.12 (s, 2H, H_{aryl}), 6.40, 5.67, 4.72, 4.46 (4 × m, 8H, NCH_2), 4.31 (s, 10H, H_{cp}), 2.2 (m, 4H, 2 NCH_2CH_2 and 2 CH_2CH_3), 1.8 (m, 2H, CH_2CH_3), 1.6 (m, 6H, 2 NCH_2CH_2 and 4 CH_2CH_3), 1.3 (m, 2H, NCH_2CH_2), 1.01, 0.94 (2 × t, $^3J_{HH}$ = 7.1 Hz, 12H, CH_2CH_3), 0.95 (m, 2H, NCH_2CH_2). $^{13}C\{^1H\}$ NMR (C_6D_6, 100 MHz, 283 K): δ 224.5 (CO), 205.2 ($C_{carbene}$), 132.5, 131.7 (2 × C_{aryl}), 90.4 (C_{aryl}–H), 80.1 (C_{cp}), 52.3, 49.2 (2 × NCH_2), 33.0, 32.8 (2 × NCH_2CH_2), 21.2, 20.3 (2 × CH_2CH_3), 14.9, 14.5 (2 × CH_2CH_3). IR (CH_2Cl_2, cm^{-1}): 1941 ν(CO). Anal. Calcd. for $C_{36}H_{48}Fe_2I_2N_4O_2$ (934.29): C 46.28, H 5.18, N 6.00. Found: C 46.33, H 5.27, N 5.86.

Complex 3a. To a suspension of benzdiimidazolium salt **1** (0.46 g, 1.0 mmol) in acetonitrile (20 mL) was added Ag_2O (0.23 g, 1.0 mmol). The mixture was stirred at 40 °C for 16 h protected from light. After solvent evaporation, the residual solid was suspended in dry CH_2Cl_2 and $[RuCl_2(\eta^6\text{-}p\text{-cymene})]_2$ (0.61 g, 1.0 mmol) was added. The suspension was stirred for 16 h and evaporated to dryness. The residue was taken up in acetone, filtered through a short pad of silica, and subsequently purified by precipitation from CH_2Cl_2–pentane. This afforded **3a** as an orange solid (0.80 g, 81%). X-Ray quality crystals were grown by slow diffusion of Et_2O into a 1,2-dichloroethane solution of **3a** at –20 °C. ^{1}H NMR ($CDCl_3$, 500 MHz, RT): δ 7.27 (s, 2H, H_{aryl}), 5.52, 5.18 (2 × d, $^3J_{HH}$ = 5.8 Hz, 8H, H_{cym}), 4.91, 4.42 (2 × m, 8H, NCH_2), 2.99 (sept, $^3J_{HH}$ = 6.9 Hz, 2H, $CHMe_2$), 2.23, 1.85 (2 × m, 8H, NCH_2CH_2), 2.04 (s, 6H, C_{cym}–CH_3), 1.63, 1.51 (2 × m, 8H, CH_2CH_3), 1.29 (d, $^3J_{HH}$ = 6.9 Hz, 12H, $CH(CH_3)_2$), 1.06 (t, $^3J_{HH}$ = 7.4 Hz, 12H, CH_2CH_3). $^{13}C\{^1H\}$ NMR ($CDCl_3$, 125 MHz, RT): δ 192.3 ($C_{carbene}$), 132.1 (C_{aryl}), 109.3 (C_{cym}–*i*Pr), 99.7 (C_{cym}–Me), 91.9 (C_{aryl}–H), 86.8, 83.6 (2 × C_{cym}–H), 50.3 (NCH_2), 32.2 (NCH_2CH_2), 30.9 ($CHMe_2$), 22.7 ($CH(CH_3)_2$), 20.5 (CH_2CH_3), 18.9 (C_{cym}–CH_3), 14.1 (CH_2CH_3). Anal. Calcd for $C_{44}H_{66}Cl_4N_4Ru_2$ (994.97) × 0.25 CH_2Cl_2: C 52.30, H 6.60, N 5.51. Found: C 52.26, H 6.58, N 5.76.

Complex 3b. To a solution of complex **3a** (50 mg, 50 µmol) in a 1 : 1 mixture of CH_2Cl_2–acetone (4 mL) was added NaBr (0.1 g, large excess). After stirring for 4 h at RT, the volatiles were evaporated and the solid residue was purified by column chromatography (Silica, eluent: CH_2Cl_2–acetone 95 : 5), yielding the title product in quantitative yield (59 mg). Recrystallization from CH_2Cl_2–pentane at –20 °C gave analytically pure orange crystals. ^{1}H NMR ($CDCl_3$, 400 MHz, RT): δ 7.29 (s, 2H, H_{aryl}), 5.61, 5.16 (2 × d, $^3J_{HH}$ = 5.8 Hz, 8H, H_{cym}), 5.03, 4.41 (2 × br, 8H, NCH_2), 3.14 (sept, $^3J_{HH}$ = 6.9 Hz, 2H, $CHMe_2$), 2.25, 1.85 (2 × br, 8H, NCH_2CH_2), 1.96 (s, 6H, C_{cym}–CH_3), 1.64, 1.51 (2 × br, 8H, CH_2CH_3), 1.29 (d, $^3J_{HH}$ = 6.9 Hz, 12H, $CH(CH_3)_2$), 1.06 (t, $^3J_{HH}$ = 7.3 Hz, 12H, CH_2CH_3). $^{13}C\{^1H\}$ NMR ($CDCl_3$, 100 MHz, RT): δ 191.1 ($C_{carbene}$), 132.2 (C_{aryl}), 110.3 (C_{cym}–*i*Pr), 99.9 (C_{cym}–Me), 92.1 (C_{aryl}–H), 87.6, 82.7 (2 × C_{cym}–H), 51.4 (NCH_2), 32.1 (NCH_2CH_2), 31.0 ($CHMe_2$), 22.7 ($CH(CH_3)_2$), 20.3 (CH_2CH_3), 19.1 (C_{cym}–CH_3), 14.1 (CH_2CH_3). Anal. Calcd for $C_{44}H_{66}Br_4N_4Ru_2$ (1172.78): C 45.06, H 5.67, N 4.78. Found: C 45.03, H 5.67, N 4.84.

Complex 5. The procedure was identical to the preparation of complex **2**, starting from dibutylimidazolium bromide **4** (0.52 g, 2 mmol), LiHMDS (1 M in THF, 2.0 mL, 2 mmol) and $[FeI(cp)(CO)_2]$ (0.58 g, 1.9 mmol). The product was obtained as a green waxy solid, which crystallized from CH_2Cl_2–pentane at –20 °C (0.28 g, 32%). ^{1}H NMR (C_6D_6, 400 MHz, 283 K): δ 6.51, 6.29 (2 × s, 2H, H_{imi}), 5.0, 4.4, (2 × br m, 2H, NCH_2), 4.15 (s, 5H, H_{cp}), 4.0, 3.7 (2 × br m, 2H, NCH_2), 1.8 (br, 1H, NCH_2CH_2), 1.5–1.1 (br, 7H, 3 NCH_2CH_2 and 4 CH_2CH_3), 0.9, 0.8 (2 × br, 6H, CH_2CH_3). $^{13}C\{^1H\}$ NMR (C_6D_6, 100 MHz, 283 K): δ 225.0 (CO), 185.6 ($C_{carbene}$), 122.3 (C_{imi}), 80.3 (C_{cp}), 53.8, 51.1 (2 × NCH_2), 33.5 (NCH_2CH_2), 20.3 (CH_2CH_3), 14.2 (CH_2CH_3). IR (CH_2Cl_2, cm^{-1}): 1935 ν(CO). Anal. Calcd. for $C_{17}H_{25}FeIN_2O$ (456.14): C 44.76, H 5.52, N 6.14. Found: C 45.03, H 5.48, N 6.08.

Complex 6a. To a solution of **4** (1.12 g, 4.3 mmol) in CH_2Cl_2 (15 mL) was added Ag_2O (0.75 g, 3.2 mmol). After stirring for 2 h at RT shielded from light, the resulting suspension was filtered through Celite and $[RuCl_2(\eta^6\text{-}p\text{-cymene})]_2$ (1.18 g, 1.9 mmol) was added. The mixture was stirred for 16 h and evaporated to dryness. The product was purified by gradient column chromatography (SiO_2, eluent: first CH_2Cl_2, then CH_2Cl_2–acetone 92 : 8), thus affording **6a** as an orange solid (1.18 g, 64%). ^{1}H NMR ($CDCl_3$, 400 MHz): δ 7.05 (s, 2H, H_{imi}), 5.36, 5.05 (2 × d, $^3J_{HH}$ = 5.9 Hz, 4H, H_{cym}), 4.56, 3.96 (2 × br, 4H, NCH_2), 2.88 (sept, $^3J_{HH}$ = 6.9 Hz, 1H, $CHMe_2$), 2.02 (s, 3H, C_{cym}–CH_3), 1.93, 1.64 (2 × br, 4H, NCH_2CH_2), 1.39 (br, 4H, CH_2CH_3), 1.23 (d, $^3J_{HH}$ = 6.9 Hz, 6H, $CH(CH_3)_2$), 0.94 (t, $^3J_{HH}$ = 7.3 Hz, 6H, CH_2CH_3). $^{13}C\{^1H\}$ NMR ($CDCl_3$, 100 MHz): δ 173.2 ($C_{carbene}$), 121.7 (C_{imi}), 107.8 (C_{cym}–*i*Pr), 99.3 (C_{cym}–Me), 85.2, 82.9 (2 × C_{cym}–H), 51.3 (NCH_2), 33.9 (NCH_2CH_2), 30.8 ($CHMe_2$), 22.7 ($CH(CH_3)_2$), 20.3 (CH_2CH_3), 18.7 (C_{cym}–CH_3), 14.1 (CH_2CH_3). Anal. Calcd. for $C_{21}H_{34}Cl_2N_2Ru$ (486.48) × 1/8 CH_2Cl_2: C 51.04, H 6.94, N 5.64. Found: C 51.03, H 6.65, N 5.82.

Complex 6b. To a solution of **6a** (50 mg, 0.1 mmol) in deoxygenated acetone was added an excess of KBr. After stirring for 4 h at RT, the resulting suspension was filtered through a short pad of Silica. Evaporation of the solvent and subsequent

http://doc.rero.ch

recrystallization from CH_2Cl_2–pentane at −20 °C gave analytically pure orange crystals. ^{1}H NMR ($CDCl_3$, 400 MHz): δ 7.09 (s, 2H, H_{imi}), 5.47, 5.05 (2 × d, $^3J_{HH}$ = 5.8 Hz, 4H, H_{cym}), 4.70, 3.93 (2 × br, 4H, NCH_2), 3.06 (sept, $^3J_{HH}$ = 6.9 Hz, 1H, $CHMe_2$), 1.98 (s, 3H, C_{cym}–CH_3), 1.97, 1.64 (2 × br, 4H, NCH_2CH_2), 1.48, 1.40 (2 × br, 4H, CH_2CH_3), 1.25 (d, $^3J_{HH}$ = 6.9 Hz, 6H, $CH(CH_3)_2$), 0.97 (t, $^3J_{HH}$ = 7.3 Hz, 6H, CH_2CH_3). ^{13}C{^{1}H} NMR ($CDCl_3$, 100 MHz): δ 171.8 ($C_{carbene}$), 122.0 (C_{imi}), 109.1 (C_{cym}–*i*Pr), 99.4 (C_{cym}–Me), 86.2, 81.9 (2 × C_{cym}–H), 52.6 (NCH_2), 33.9 (NCH_2CH_2), 30.9 ($CHMe_2$), 22.8 ($CH(CH_3)_2$), 20.2 (CH_2CH_3), 19.0 (C_{cym}–CH_3), 14.1 (CH_2CH_3). Anal. Calcd. for $C_{21}H_{34}Br_2N_2Ru$ (575.39): C 43.84, H 5.96, N 4.87. Found: C 43.99, H 5.95, N 4.73.

Electrochemical measurements

Electrochemical studies were carried out using an EG & G Princeton Applied Research Potentiostat Model 273A employing a gas-tight three electrode cell under an argon atmosphere. A platinum disk with 3.8 mm^2 surface area was used as the working electrode and was polished before each measurement. The reference electrode was Ag/AgCl, the counter electrode was a Pt wire. In all experiments, Bu_4NPF_6 (0.1 M in dry CH_2Cl_2) was used as supporting electrolyte with analyte concentrations of approximately 1 mM. Measurements were performed at 100 mV s^{-1} scan rates. The redox potentials were referenced to ferrocenium/ferrocene (Fc^+/Fc; $E_{1/2}$ = 0.46 V *vs.* SCE)[13] or to $[Ru(bpy)_3]^{3+}/[Ru(bpy)_3]^{2+}$ ($E_{1/2}$ = 1.39 V *vs.* SCE)[14] as internal standards.

Crystal structure determinations of complexes 2, 3a, and 6b

Suitable single crystals were mounted on a Stoe Mark II-Imaging Plate Diffractometer System (Stoe & Cie, 2002) equipped with a graphite-monochromator. Data collection was performed at −100 °C using Mo-Kα radiation (λ = 0.71073 Å) with a nominal crystal to detector distance of 100 mm (for **2**) and 135 mm (for **3a** and **6b**), respectively. All structures were solved by direct methods using the program SHELXS-97 and refined by full matrix least squares on F^2 with SHELXL-97.[15] The hydrogen atoms were included in calculated positions and treated as riding atoms using SHELXL-97 default parameters. A partial disorder was found for the CO and I atoms in complex **2**. About 5% of the I is situated near the CO group and the CO group is consequently 95% occupied. It was not possible to model the disorder for the 5% occupied CO group sharing the space with the 95% occupied I. Therefore no 95/5% disorder was modelled for the entire part of the structure and instead, an EADP was applied to the CO group assuming 100% occupancies of CO and I. Complex **3a** crystallizes with one disordered Et_2O molecule (75% occupancy) per asymmetric unit. The thermal parameters have been set equal for the partially occupied atoms in the two parts of the disordered molecule. For all structures, the non-hydrogen atoms were refined anisotropically. A semi-empirical absorption correction was applied using MULscanABS as implemented in PLATON03.[16]

Crystal data for 2. Empirical formula $[Fe_2I_2(CO)_2(C_{34}H_{48}N_4)\cdot 4CH_2Cl_2]$, M 1273.99, green plate, monoclinic, space group $P2_1/c$ (no. 14), a = 11.3269(10) Å, b = 12.2366(6) Å, c = 18.2520(15) Å, β = 98.195(7)°, V = 2503.9(3) Å^3, Z = 2, D_c = 1.690 g cm^{-3}, Mo-Kα radiation, λ = 0.71073 Å, T = 173(2) K, 27277 reflections measured, 6768 unique (R_{int} = 0.0444). Final GooF = 1.062, R_1 = 0.448, wR_2 = 0.1095, R indices based on 6768 reflections with $I > 2\sigma(I)$ (refinement on F^2), 264 parameters, 0 restraints. Lp and absorption corrections applied, μ = 2.277 mm^{-1}. CCDC number: 680401.

Crystal data for 3a. Empirical formula $[Ru_2Cl_4(C_{44}H_{66}N_4)\cdot 1.5C_4H_{10}O]$, M 1139.24, orange plate, monoclinic, space group $P2_1/c$ (no. 14), a = 11.6954(7) Å, b = 7.1268(3) Å, c = 34.419(2) Å, β = 91.422(5)°, V = 2868.0(3) Å^3, Z = 2, D_c = 1.281 g cm^{-3}, Mo-Kα radiation, λ = 0.71073 Å, T = 173(2) K, 28304 reflections measured, 5106 unique (R_{int} = 0.1066). Final GooF = 1.131, R_1 = 0.0570, wR_2 = 0.1637, R indices based on 5106 reflections with $I > 2\sigma(I)$ (refinement on F^2), 272 parameters, 4 restraints. Lp and absorption corrections applied, μ = 0.749 mm^{-1}. CCDC number: 680402.

Crystal data for 6b. Empirical formula $[RuBr_2(C_{21}H_{34}N_2)]$, M 575.39, orange rod, monoclinic, space group $P2_1/n$ (no. 14), a = 17.9231(8) Å, b = 12.3593(4) Å, c = 20.8012(11) Å, β = 91.923(4)°, V = 4605.2(4) Å^3, Z = 8, D_c = 1.660 g cm^{-3}, Mo-Kα radiation, λ = 0.71073 Å, T = 173(2) K, 46581 reflections measured, 8198 unique (R_{int} = 0.0463). Final GooF = 0.937, R_1 = 0.0256, wR_2 = 0.0503, R indices based on 8198 reflections with $I > 2\sigma(I)$ (refinement on F^2), 479 parameters, 0 restraints. Lp and absorption corrections applied, μ = 4.159 mm^{-1}. CCDC number: 690656.

Results

Synthesis of complexes

The benzdiimidazolium ligand precursor **1** was synthesised according to a procedure described previously by Bielawski and coworkers.[10] Double metallation of **1** with Fe^{II} centers was accomplished in analogy to the synthesis of monometallic carbene complexes *via* the free-carbene route (Scheme 2).[6] Hence, deprotonation of **1** with $LiN(SiMe_3)_2$ followed by addition of [FeI(cp)(CO)$_2$] as the iron(II) precursor afforded, after irradiation, complex **2** as a moderately air-stable complex. The analogous dinuclear ruthenium(II) complex **3a** was prepared by transmetallation of the corresponding Ag_2-complex.[17] Despite the low solubility of the diimidazolium precursor, treatment of **1** with 1 moleq Ag_2O and subsequent addition of $[RuCl_2(cymene)]_2$ produced complex **3a** as an air-stable, orange solid in good overall yield (81% from **1**). Halide exchange at the ruthenium centers in order to prepare **3b** was performed by a metathesis reaction using excess NaBr. For comparative purposes, the corresponding monometallic complexes **5** and **6** were prepared by analogous methods starting from the dibutyl imidazolium salt **4** (Scheme 2).

Complexes **2** and **3** were fully analysed both in solution and in the solid state. A characteristic feature of the NMR spectra is the magnetic inequivalence of the two protons of the *N*-bound methylene group. In complex **2**, this leads to 4 different signals owing to the asymmetric metal center (benzene solution). Line broadening, yet no coalescence was observed at 60 °C, indicating that the iron–carbene bond is relatively rigid and that rotation is slow on the NMR time scale. In analogy, the corresponding monometallic complex **5** displays also 4 inequivalent signals

http://doc.rero.ch

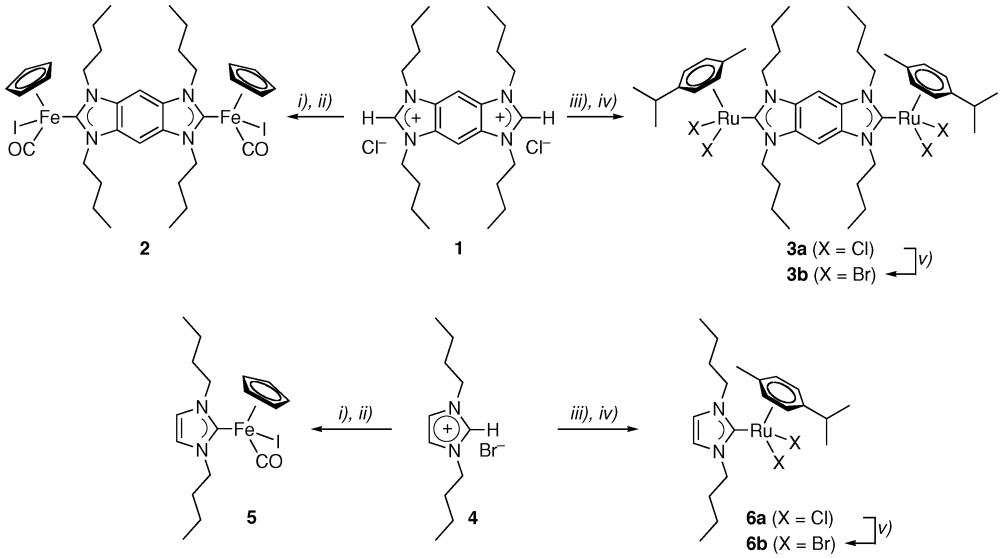

Scheme 2 Synthesis of the complexes; reagents and conditions: (i) $LiN(SiMe_3)_2$, thf; then $[FeI(cp)(CO)_2]$, toluene; (ii) *hν*, CH_2Cl_2; (iii) Ag_2O, MeCN, 40 °C; (iv) $[RuCl_2(cymene)]_2$, CH_2Cl_2;(v) NaBr, CH_2Cl_2–acetone.

http://doc.rero.ch

for the methylene protons. As a consequence of the smaller carbene ligand, however, coalescence of these signals into a single resonance occurs at T_{coal} = 303(±3) K, corresponding to an approximate barrier of rotation about the Fe–$C_{carbene}$ bond $\Delta G^{\ddagger}$ = 58.6(±0.6) kJ mol^{-1}. Notably, cooling of a solution of the dimetallic complex **2** in CD_2Cl_2 to −10 °C produces 8 well-separated signals in the 6–3.8 ppm range for the methylene protons. At this temperature, differentiation between the racemic and the *meso* conformations due to the presence of two chiral iron centers apparently becomes possible.

In the Ru_2-complex **3a**, the signals due to the nitrogen-bound methylene protons merge into two multiplets centered at δ_H 4.91 and 4.42, respectively. This behavior is consistent with a restricted rotation about the N–C_{butyl} bond, presumably due to the pronounced steric impact of the cymene ligand. The cymene protons appear as a single set of resonances and suggest that the metal centers are symmetry related. Notably, coalescence of the corresponding signals of the monoruthenium complex **6a** (δ_H 4.56 and 3.96) occurs at T_{coal} = 311(±3) K. The associated activation energy, $\Delta G^{\ddagger}$ = 58.6(±0.6) kJ mol^{-1}, is identical with that determined for the iron analogue **5**.

The structures deduced in solution are also preserved in the solid state, as confirmed by X-ray diffraction analyses of single crystals of **2** and **3a**. The molecular structures (Fig. 1) show the expected connectivity patterns. In both complexes, the metal centers are crystallographically related by symmetry. The pertinent bond lengths in the dimetallic complexes do not deviate particularly as compared with related monometallic complexes (Table 1). A Fe···Fe distance of 10.591(1) Å has been determined for **2**, while in **3a** the longer Ru–$C_{carbene}$ bond due to the larger radius of the ruthenium ion results in a slightly larger metal–metal separation (Ru···Ru 10.757(1) Å).

The data from a crystal structure determination of the monometallic ruthenium complex **6b** (Fig. 1) indicate that the Ru–carbene bond length is slightly longer in the $RuBr_2$ complex **6b** as compared to the $RuCl_2$ system **3a**.

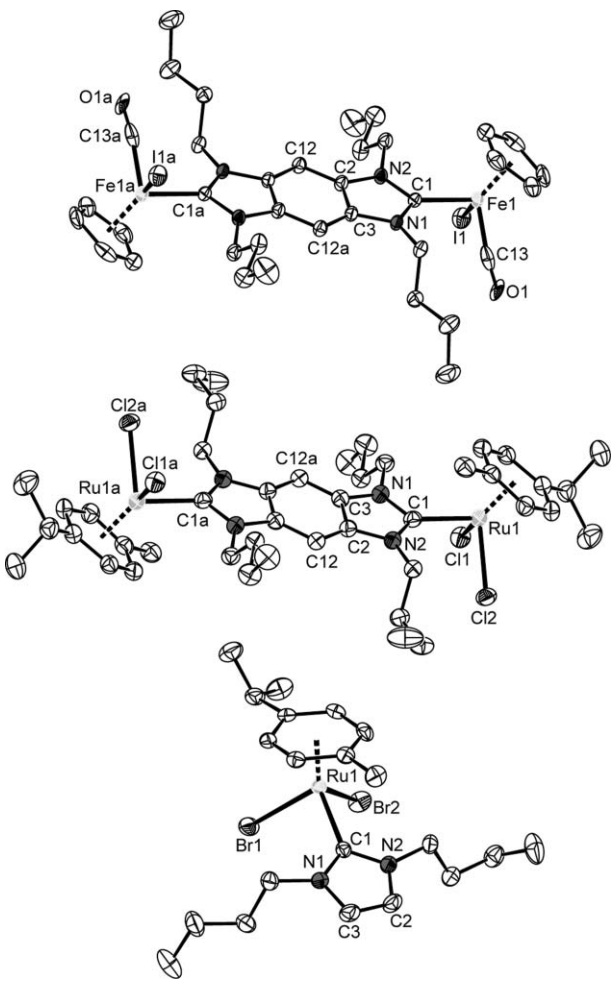

Fig. 1 ORTEP representation of **2** (top; 50% probability) and **3a** (middle; 30% probability) and **6b** (bottom, only one of the two molecules in the asymmetric unit shown; 50% probability). Hydrogen atoms and cocrystallised solvents were omitted for clarity.

Table 1 Selected bond lengths (Å) of complexes **2**, **3a**, and **6b**

Complex	**2** (M = Fe, X = I)	**3a** (M = Ru, X = Cl)	**6b**[a] (M = Ru, X = Br)
M1–C1	1.969(3)	2.065(4)	2.084(3)
M1–X1	2.6475(6)	2.4120(11)	2.5640(4)
M1–X2[b]	1.769(5)	2.4130(11)	2.5556(4)
M1–$C_{centroid}$	1.728(2)	1.687(2)	1.691(1)
C1–N1	1.356(4)	1.366(5)	1.361(4)
C1–N2	1.367(4)	1.363(5)	1.360(4)
N1–C3	1.398(4)	1.399(5)	1.375(4)
N2–C2	1.391(4)	1.394(5)	1.383(4)
C2–C3	1.407(4)	1.395(6)	1.328(5)
C2–C12	1.387(4)	1.381(6)	—
C3–C12a	1.386(4)	1.392(5)	—
M1 ··· M1a	10.591(1)	10.7563(8)	—

[a] Values are given only for one of the two molecules in the asymmetric unit of **6b**; the bond lengths are identical within esd's for both molecules. [b] X2 = C13 for complex **2**.

Table 2 Electrochemical data for the complexes **2**, **3**, **5**, and **6**

Complex	Metal system	$E_{1/2}$/V	ΔE/mV	$\Delta E_{1/2}$/mV	K_c
2	Fe_2	+0.50, +0.58[a,c]	143	80	22.5
3a	Ru_2	+1.15, +1.21[b,c]	119	58	9.6
3b	Ru_2	+1.13, +1.17[b,c]	129	42	5.1
5	Fe	+0.42[a]	99	—	—
6a	Ru	+1.09[b]	85	—	—
6b	Ru	+1.08[b]	97	—	—

[a] Measurements in CH_2Cl_2 using $[NBu_4]PF_6$ as supporting electrolyte; potentials *vs.* SCE referenced to $[Ru(bpy)_3]^{3+}/[Ru(bpy)_3]^{2+}$ ($E_{1/2}$ = +1.39 V, ΔE = 112(±7) mV) as internal standard. [b] *vs.* SCE, Fc^+/Fc ($E_{1/2}$ = +0.46 V, ΔE = 113(±7) mV) as internal standard. [c] Peak potentials determined by deconvolution of the signal from DPV.

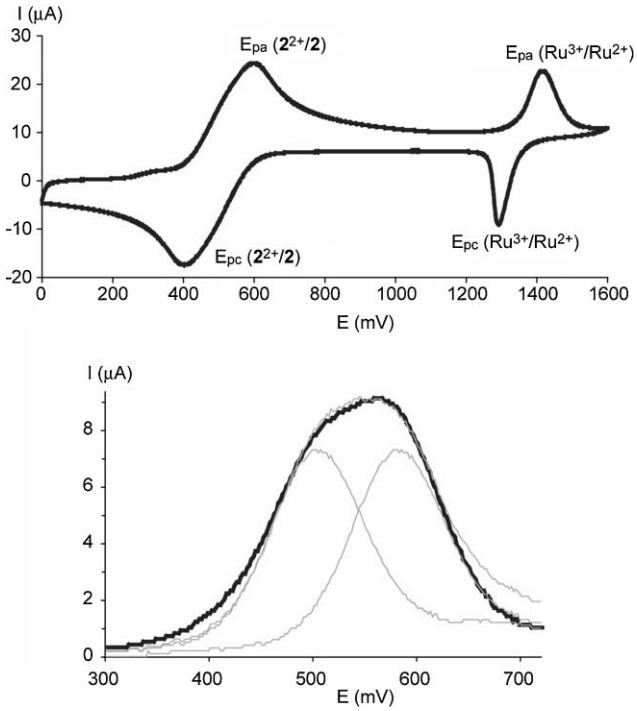

Fig. 2 Cyclic voltammetry diagram of complex **2** (top, $[Ru(bpy)_3]^{2+}$ as internal reference, denoted as Ru^{3+}/Ru^{2+}) and relevant section of the differential pulse voltammetry analysis of complex **2** (bottom) depicting the measured data (bold line), and the convoluted curve obtained from adding two potential-shifted and weighted DPV signals of the monometallic complex **5** (grey lines).

Electrochemical properties

Electrochemical measurements were carried out in order to determine whether the two dicarbene-linked metal centers are electronically coupled. In MeCN, several oxidation processes were observed even for the monometallic complexes **6a** and **6b**, some of which appeared to be irreversible. This suggests partial formation of the corresponding solvento complexes, in which a metal-bound halide is replaced by a coordinating MeCN molecule. Therefore, electrochemical measurements were generally performed in CH_2Cl_2 solution, where halide dissociation is less favored. Cyclic voltammetry (CV) measurements indicate that, in CH_2Cl_2, complex **2** undergoes a single reversible oxidation with $E_{1/2}$ = +0.54 V (Fig. 2a, Table 2). This potential compares well with the redox-potential of the monometallic carbene complex **5** and indicates a metal- rather than a ligand-centered redox process. Differential pulse voltammetry (DPV) reveals that the oxidation signal is significantly broader than that of the monometallic species. Signal deconvolution using the DPV curve of the monocarbene complex **5** yields two oxidations that are separated by ΔE = 80 mV (Fig. 2b). This relatively small separation of the oxidation potentials hampered our attempts to stabilize and characterize the mixed-valent Fe^{II}/Fe^{III} intermediate. The measured separation of the oxidation potentials corresponds to a comproportionation constant K_c = 22.5, thus reflecting a weak intermetallic interaction. According to the Robin and Day classification,[18] complex **2** corresponds to a class II system and hence represents a molecular switch with two mutually dependent redox sites.

The dinuclear ruthenium systems **3a** and **3b** display a considerably sharper reversible oxidation at $E_{1/2}$ = +1.18 V and +1.15 V, respectively (CV measurements). No further oxidation was observed up to +1.6 V.† Concentration-dependent analysis of the bimetallic complex **3a** and the monometallic analogue **6a** indicated a persistent 1.7 : 1 ratio of the anodic peak current over the measured concentration range (0.5–3 mM). Taking into account the slightly different diffusion coefficients of **3a** and **6a**, this ratio is in good agreement with a two-electron oxidation process in **3**. Experiments using DPV revealed only a small broadening as compared to the related monometallic reference complexes **6**. The signal can be deconvoluted analogous to that of **2** (see above) and affords two bands that are separated by 58 mV and 42 mV for **3a** and **3b**, respectively.† The latter value is very close to the statistically expected separation of a bifunctional system containing two fully independent redox-active sites.[19]

Accordingly, the ruthenium centers in **3** experience weaker mutual coupling than the iron centers in **2** and are, in particular in complex **3b** essentially decoupled (class I system).

Attempts to detect and characterize the surmised mixed-valent intermediates have been unsuccessful. Spectroelectrochemical analyses using an optically transparent thin-layer electrochemical cell[20] only allowed for identifying the pertinent absorbance

http://doc.rero.ch

properties of the parent Ru^{II}/Ru^{II} complex **3** (CT band at λ_{max} = 336 nm) and those of the fully oxidized Ru^{III}/Ru^{III} species $[\mathbf{3}]^{2+}$ (λ_{max} = 315 nm). Notably, the absorption characteristics of **3** differ from those obtained after exposure of complex **3** to high potentials (1.5 V) for 10 min and subsequent reduction. The 21 nm hypsochromic shift of λ_{max} suggests a slow chemical reaction following the electrochemical oxidation (EC mechanism), which may limit the chemical accessibility of the Ru^{III}/Ru^{III} complex $[\mathbf{3}]^{2+}$.

Discussion

The weak intermetallic charge transfer in **2** may seem remarkable when assuming a supposedly fully conjugated π system in the benzodicarbene spacer ligand. Since the M–$C_{carbene}$ bond in Fe–NHC complexes is known to have some π character,[6] we surmise the weak coupling being due to only very limited conjugation between the heterocyclic NCN amidinylidene moiety and the central arene fragment of the ligand. A small overlap of these two π systems will ensue weak charge delocalization within the dicarbene spacer ligand. This model is supported by theoretical analyses of metal–carbene complexes,[21] which suggest that, in a first approximation, the NHC ligand may be electronically split into a three-center-four-electron NCN unit and an olefinic C=C part with relatively small mutual overlap (**B**, Scheme 3). The contribution of resonance structure **C** comprising a fully delocalized π electron system was calculated to be only of minor relevance. This is in line with deuteration and chlorination experiments, which proceed in carbenes but not in imidazolium salts.[22] Significantly, the impact of benzimidazolylidenes on the metal center is reported to correspond to saturated imidazolinylidene ligands rather than to unsaturated imidazolylidenes,[23] thus corroborating the notion of weak orbital overlap between the benzene fragment and the carbenic NCN donor site.

Scheme 3 Resonance structures generally used for describing *N*-heterocyclic carbene–metal complexes.

The generally weaker metal–metal coupling in the ruthenium complexes **3** as opposed to the iron system **2** requires a differentiation that does not rely on intrinsic ligand properties. Electronic coupling is expected to strongly depend on the M–$C_{carbene}$ bond strength. According to calculations, the metal–carbene bond is dominated by electrostatic forces (ΔV_{elst} *ca.* 70%), while the covalent term is typically low (ΔE_{orb} around 30%).[21] The electrostatic attraction between the carbene ligand and the naturally electron-rich ruthenium should be weaker than with relatively electron-poor iron. This effect is further amplified by the ancillary ligands, as the iron site comprises a CO while the $[RuCl_2(cymene)]$ fragment lacks strong π acids. Such considerations may be particularly relevant in the mixed-valent intermediate, comprising an M^{III} center. While such a model provides a rationale for the observed differences for intramolecular metal–metal coupling with these ditopic carbene ligands, further studies are clearly needed for substantiating this concept.

Conclusions

The potential of dicarbene ligands as spacers for interconnecting redox-active metal centers has been probed by analyzing the electrochemical properties of bimetallic iron and ruthenium complexes. While in the ruthenium complexes, metal–metal interactions are very weak, we found evidence of modest coupling in the di-iron complex. These results suggest that the use of ditopic carbene ligands combined with a careful choice of metal centers and ancillary ligands may provide access to novel and useful materials for application in molecular electronics.

Acknowledgements

This work has been supported by the Swiss National Science Foundation. M. A. gratefully acknowledges an Assistant Professorship from the Alfred Werner Foundation.

Notes and references

1 N-*heterocyclic carbenes in synthesis*, ed. S. P. Nolan, Wiley-VCH, Weinheim, 2006; R. H. Crabtree, *Coord. Chem. Rev.*, 2007, **251**, 595; E. A. B. Kantchev, C. J. O'Brien and M. G. Organ, *Angew. Chem., Int. Ed.*, 2007, **46**, 2768; A. T. Normand and K. J. Cavell, *Eur. J. Inorg. Chem.*, 2008, 2781.

2 A. J. Boydston, K. A. Williams and C. W. Bielawski, *J. Am. Chem. Soc.*, 2005, **127**, 12496; T. Sajoto, P. I. Djurovich, A. Tamayo, M. Yousufuddin, R. Bau, M. E. Thompson, R. J. Holmes and S. R. Forrest, *Inorg. Chem.*, 2005, **44**, 7992.

3 D. Bourissou, O. Guerret, F. Gabbai and G. Bertrand, *Chem. Rev.*, 2000, **100**, 39; W. A. Herrmann, *Angew. Chem., Int. Ed.*, 2002, **41**, 1290; M. Lee and C. Hu, *Organometallics*, 2004, **23**, 976.

4 π interactions have also been evidenced for a number of other metals; for examples, see: X. Hu, I. Castro-Rodriguez, K. Olsen and K. Meyer, *Organometallics*, 2004, **23**, 755; D. Nemcsok, K. Wichmann and G. Frenking, *Organometallics*, 2004, **23**, 3640.

5 A. J. Arduengo, S. F. Gamper, J. C. Calabrese and F. Davidson, *J. Am. Chem. Soc.*, 1994, **116**, 4391; A. D. D. Tulloch, A. B. Danopoulos, S. Kleinhenz, M. E. Light, M. B. Hursthouse and G. Eastham, *Organometallics*, 2001, **20**, 2027; S. Saravankumar, A. I. Oprea, M. K. Kindermann, P. G. Jones and J. Heinicke, *Chem.–Eur. J.*, 2006, **12**, 3143; W. A. Herrmann, J. Schütz, G. D. Frey and E. Herdtweck, *Organometallics*, 2006, **25**, 2437; D. S. McGuinness, N. Saendig, B. F. Yates and K. J. Cavell, *J. Am. Chem. Soc.*, 2001, **123**, 4029.

6 L. Mercs, G. Labat, A. Neels, A. Ehlers and M. Albrecht, *Organometallics*, 2006, **25**, 5648.

7 D. M. Khramov, V. M. Lynch and C. W. Bielawski, *Organometallics*, 2007, **26**, 6042.

8 J.-P. Sauvage, J.-P. Collin, J.-C. Chambron, S. Guillerez, C. Coudret, V. Balzani, F. Barigelletti, L. De Cola and L. Flamigni, *Chem. Rev.*, 1994, **94**, 993; S. Barlow and D. O'Hare, *Chem. Rev.*, 1997, **97**, 637; F. Barigelletti, L. Flamigni, J.-P. Collin and J.-P. Sauvage, *Chem. Commun.*, 1997, 333; F. Paul and C. Lapinte, *Coord. Chem. Rev.*, 1998, **178**, 427; B. Bosnich, *Inorg. Chem.*, 1999, **38**, 2554; R. Dembinski, T. Bartik, B. Bartik, M. Jaeger and J. A. Gladysz, *J. Am. Chem. Soc.*, 2000, **122**, 810.

9 H. M. McConnell, *J. Chem. Phys.*, 1961, **35**, 508.

10 D. M. Khramov, A. J. Boydston and C. W. Bielawski, *Angew. Chem., Int. Ed.*, 2006, **45**, 6186; A. J. Boydston, D. M. Khramov and C. W. Bielawski, *Tetrahedron Lett.*, 2006, **47**, 5123.

11 A. R. Chianese, A. Kovacevic, B. M. Zeglis, J. W. Faller and R. H. Crabtree, *Organometallics*, 2004, **23**, 2461.

12 S. S. Palimkar, S. A. Siddiqui, T. Daniel, R. J. Lahoti and K. V. Srinivasan, *J. Org. Chem.*, 2003, **68**, 9371.

13 N. G. Connelly and W. E. Geiger, *Chem. Rev.*, 1996, **96**, 877.

14 Determined using ferrocenium/ferrocene (Fc^+/Fc) couple ($E_{1/2}$ = 0.46 V *vs.* SCE).

15 G. M. Sheldrick, *Acta Crystallogr., Sect. A: Found. Crystallogr.*, 2008, **64**, 112.

16 A. L. Spek, *J. Appl. Crystallogr.*, 2003, **36**, 7.

http://doc.rero.ch

17 M. J. Wang and I. J. B. Lin, *Organometallics*, 1998, **17**, 972; A. R. Chianese, X. Li, M. C. Janzen, J. W. Faller and R. H. Crabtree, *Organometallics*, 2003, **22**, 1663; J. C. Garrison and W. J. Youngs, *Chem. Rev.*, 2005, **105**, 3978.
18 M. B. Robin and P. Day, *Adv. Inorg. Chem. Radiochem.*, 1967, **10**, 247.
19 For a system comprising two one-electron redox processes, the relationship $\Delta\Delta G^\circ = -RT\ln(K) = nF\Delta\Delta E^\circ$ can be rearranged to $\Delta\Delta E^\circ = \log(K) \times 59\,\text{mV}$ (with $T = 298\,\text{K}$, $n = 1$, $K = K_c$). In a system comprising two identical yet independently operating redox-active centers that undergo a one-electron redox process, the macroscopic equilibrium constant $K = 4$, and hence, $\Delta\Delta E^\circ = 36\,\text{mV}$.
20 M. Krejcik, M. Danek and F. Hartl, *J. Electroanal. Chem.*, 1991, **317**, 179.
21 R. Tonner, G. Heydenrych and G. Frenking, *Chem.–Asian J.*, 2007, **2**, 1555; E. F. Penka, C. W. Schläpfer, M. Atanasov, M. Albrecht and C. Daul, *J. Organomet. Chem.*, 2007, **692**, 5709; M. Tafipolsky, W. Scherer, K. Öfele, G. Artus, B. Pedersen, W. A. Herrmann and G. S. McGrady, *J. Am. Chem. Soc.*, 2002, **124**, 5865.
22 A. J. Arduengo, F. Davidson, H. V. R. Dias, J. R. Goerlich, D. Khasnis, W. J. Marshall and T. K. Prakasha, *J. Am. Chem. Soc.*, 1997, **119**, 742; M. K. Denk and J. M. Rodezno, *J. Organomet. Chem.*, 2001, **617**, 737.
23 Y. Liu, P. E. Lindner and D. M. Lemal, *J. Am. Chem. Soc.*, 1999, **121**, 10626; F. E. Hahn, M. Paas, D. Le Van and T. Lügger, *Angew. Chem., Int. Ed.*, 2003, **42**, 5243; F. E. Hahn, D. Le Van, M. Paas and R. Fröhlich, *Dalton Trans.*, 2006, 860.

http://doc.rero.ch